Journal of Cell Science 112, 2355-2367 (1999)
Printed in Great Britain © The Company of Biologists Limited 1999
JCS9926

Tau regulates the attachment/detachment but not the speed of motors in microtubule-dependent transport of single vesicles and organelles

B. Trinczek*, A. Ebneth‡, E.-M. Mandelkow and E. Mandelkow*

Max-Planck Unit for Structural Molecular Biology, Notkestrasse 85, D-22607 Hamburg, Germany
*Authors for correspondence (e-mail: trinczek@mpasmb.desy.de; mand@mpasmb.desy.de)
‡Present address: GENION Forschungsgesellschaft mbH, Abteistrasse 57, 20149 Hamburg, Germany

Accepted 30 April; published on WWW 24 June 1999

SUMMARY

We have performed a real time analysis of fluorescence-tagged vesicle and mitochondria movement in living CHO cells transfected with microtubule-associated protein tau or its microtubule-binding domain. Tau does not alter the speed of moving vesicles, but it affects the frequencies of attachment and detachment to the microtubule tracks. Thus, tau decreases the run lengths both for plus-end and minus-end directed motion to an equal extent. Reversals from minus-end to plus-end directed movement of single vesicles are strongly reduced by tau, but reversals in the opposite direction (plus to minus) are not. Analogous effects are observed with the transport of mitochondria and even with that of vimentin intermediate filaments. The net effect is a directional bias in the minus-end direction of microtubules which leads to the retraction of mitochondria or vimentin IFs towards the cell center. The data suggest that tau can control intracellular trafficking by affecting the attachment and detachment cycle of the motors, in particular by reducing the attachment of kinesin to microtubules, whereas the movement itself is unaffected.

Key words: Tau, Mitochondrion, Transport, Exocytosis, Intermediate filament

INTRODUCTION

Microtubules (MTs) contribute to diverse cellular processes such as cell morphogenesis, cell division and intracellular trafficking (Drubin and Nelson, 1996; Goodson et al., 1997; Hyman and Karsenti, 1996). In cells, MTs can change their lengths via dynamic instability (Waterman-Storer and Salmon, 1997) and they can serve as tracks for organelle transport mediated by MT-dependent motor proteins such as the plus-end directed motor kinesin and its relatives or the minus-end directed motor dynein (Brady, 1995; Vallee and Sheetz, 1996; Hirokawa, 1998; Lippincott-Schwartz et al., 1995). These motors can transport their cargoes towards the cell periphery or back towards the MT organizing center (MTOC), respectively, e.g. mitochondria (Morris and Hollenbeck, 1995; Tanaka et al., 1998), lysosomes (Hollenbeck and Swanson, 1990), peroxisomes (Wiemer et al., 1997), phagosomes (Blocker et al., 1998), and endocytotic or exocytotic vesicles (Presley et al., 1997; Scales et al., 1997). Kinesin is also involved in the coalignment of intermediate filaments (IFs) with MTs by triggering IF spreading along the MT tracks (Gyoeva and Gelfand, 1991; Klymkowsky, 1995; Prahlad et al., 1998).

MTs are decorated with MT-associated proteins, such as tau, microtubule-associated protein (MAP)2, or MAP4, which promote MT assembly (Hirokawa, 1994; Mandelkow and Mandelkow, 1995) and play an important role in organizing the MT cytoskeleton (Matus, 1994; Barlow et al., 1994). They share sequence homology in the conserved repeat regions located in the C-terminal MT-binding domain (Chapin and Bulinski, 1991). Their N-terminal projection domain protrudes from the MT surface and can serve as a MT spacer (Chen et al., 1992); it is variable both in amino acid composition and length. Tau is enriched in axons, MAP2 in the somatodendritic compartment of neurons (Binder et al., 1985; Kanai and Hirokawa, 1995), whereas MAP4 is ubiquitous (West et al., 1991; Chapin and Bulinski, 1991; Barlow et al., 1994). MAPs can affect the mobility of vesicles in a phosphorylation-dependent manner (Hamm-Alvarez et al., 1993; Sato-Harada et al., 1996; Bulinski et al., 1997). We have shown recently that the overexpression of tau inhibits the plus-end directed transport of vesicles along microtubules by kinesin so that the minus-end directed transport by dynein becomes more dominant (Ebneth et al., 1998). This slows down exocytosis and affects the distribution of mitochondria which become clustered near the MT organizing center. The results pointed to a physiological role of MAPs as regulators of motor protein-dependent transport. However, it remained unclear how tau might perturb the balance between plus-end and minus-end directed transport in cells, particularly since several in vitro studies had suggested that the interference of MAPs with motor-dependent movement was relatively weak (von Massow et al., 1989; Paschal et al., 1989; Hagiwara et al., 1994; Lopez and Sheetz, 1993).

This motivated us to study the transport phenomena directly by observing the movement of fluorescently tagged single vesicles and organelles in real time. We observed post-Golgi vesicles and mitochondria in living CHO (Chinese hamster ovary) cells stably transfected with tau constructs containing the microtubule-binding domain, with or without the projection domain. We assayed their effect on different parameters of motion such as velocity, run length, reversal frequency or the fraction of moving organelles. The velocity shows the activity of motors attached to microtubules, the run length reflects the detachment from microtubules, and the reversal frequency or the fraction of moving particles indicates their initial attachment. The data show that tau perturbs the balance of the bidirectional motion of the vesicles by decreasing the reversal frequency from minus-end to plus-end directed transport (inbound to outbound). Run lengths of vesicles and mitochondria were reduced to a similar degree in both directions. By assaying the fraction of actively transported mitochondria, we found that tau mainly inhibits transport towards the cell periphery. However, the velocities of the organelle transport remained unchanged, indicating that the motor activities were not altered by tau. The inhibitory effect of tau became also obvious for the kinesin-dependent spreading of IFs along microtubules. The observations argue that tau does not affect motor activity itself, but acts as a 'speed bump' where transport is halted or diverted, and as an inhibitor of motor attachment which preferentially affects kinesin.

MATERIALS AND METHODS

Tau isoforms and constructs

For transfection, we used the largest human tau isoform (htau40, 441 residues), the constructs K35 and K33, which lack most or all of the projection domain, and the tau construct K23 without the repeat domain. Their cloning, bacterial expression, purification, and binding to MTs were reported previously (see Fig. 1A; Gustke et al., 1994; Preuss et al., 1997).

Antibodies, dyes, fixation and immunofluorescence

The following antibodies were used: mouse monoclonal anti-tubulin antibody DM1A was purchased from Sigma (Deisenhofen, Germany). Polyclonal rabbit anti-HA-tag antibody and polyclonal rabbit anti-tau antibody K9JA were from DAKO (Hamburg, Germany), and anti-vimentin antibody from Boehringer Mannheim (Germany). All fluorescently (TRITC, FITC and AMCA) labeled secondary antibodies were from DIANOVA (Hamburg, Germany). MitoTracker™ Red was purchased from Molecular Probes (Eugene OR, USA). Cells were fixed with 2% paraformaldehyde and incubation with antibodies was performed as described (Preuss et al., 1995). For staining of mitochondria MitoTracker™ Red was added at a concentration of 400 nM 30 minutes before fixation. Cells were examined with an Axioplan fluorescence microscope (Zeiss, Jena, Germany) equipped with a ×100/1.4 NA oil-immersion objective and filters optimized for triple-label experiments.

Cell culture

CHO cells were grown in HAM's F12 medium supplemented with 10% fetal calf serum and 2 mM glutamine (Biochrom, Berlin, Germany). For immunofluorescence cells were seeded onto coverslips at a density of 2×10^4 cells/cm^2 in 24-well culture dishes and grown overnight at 37°C with 5% CO_2. For stable transfection, plasmids derived from pcDNA3 (Invitrogen, Leek, Netherlands) coding for htau40, K35, K33 or K23 under the control of the CMV-promoter were introduced into cells by the DOTAP-method (Boehringer Mannheim, Germany) according to the manufacturer's instructions, selected in the presence of 600 μg/ml geneticin, and subsequently recloned (tau40-cells: Preuss et al., 1995; K35- and K23-cells: Ebneth et al., 1998; K33-cells: this work). For controls CHO cells were stably mock-transfected (vector without tau). The constructs were tagged at the 5′ end with the HA-coding sequence in order to detect and quantify the different tau variants by using the same antibody (polyclonal anti-HA antibody; Field et al., 1988).

Determination of tau protein concentration in the stably transfected cells

Recombinant tau protein was prepared as described (Gustke et al., 1994) and concentrated in 25 mM Hepes, pH 7.2, 1 mM PMSF in Microcon microconcentrators (Amicon Inc., Beverly MA, USA). Different concentrations of the protein (1.9 mg/ml, 0.95 mg/ml and 0.38 mg/ml) were microinjected with an Eppendorf Micromanipulator 5171 at constant pressure within 15 minutes, and cells were then fixed in parallel with the tau stable cell lines and stained with a polyclonal anti-tau antibody. The fluorescence signal of the tau-stained cells was acquired under identical illumination conditions with a CCD-camera, quantified by using the Metamorph® software package (both from Visitron, Puchheim, Germany) and normalized to the cell's dimensions. Regression analysis of the normalized fluorescence intensities of the microinjected cells was performed with the program Sigma Plot (SPSS Inc., R = 0.9995; Fig. 1B).

Preparation of the real time experiments and data acquisition

Cells were seeded onto a LabTek chambered coverglass (NUNC, Naperville IL, USA) at 70% confluency. For monitoring exocytotic vesicles, cells were transiently transfected with GFP-VSVG (green fluorescent protein-vesicular stomatitis virus glycoprotein) vector (kindly provided by Thomas E. Kreis) by the DOTAP method, and for mitochondria, MitoTracker™ Red was added to cells at a final concentration of 200 nM and incubated for 10 minutes. Cells were rinsed with medium, and incubated for 30 minutes at 37°C and 5% CO_2. For randomizing the MT organization of the different cell lines, 5 μM nocodazole was added to the medium (to destroy microtubules), incubated for 60 minutes at 37°C and 5% CO_2, then removed by washing with medium and subsequently treated with 10 μM taxotere at 37°C and 5% CO_2 for 30 minutes (to reassemble microtubules in random orientations (DeBrabander et al., 1986; Weisshaar et al., 1992). For motion analysis of mitochondria in the tau-stable cell lines, cells were treated with nocodazole to allow the dispersion of the organelles. After 1 hour of incubation at 37°C the drug was removed by washing steps, and the cells were subsequently analyzed under the microscope after the MT network was rebuilt (typically 15 minutes after washing). Chambered coverglasses were sealed with Baysilone (Bayer, Leverkusen, Germany) to keep the pH of medium under the microscope constant at pH 7.2-7.4 (typically for 1 hour to 2 hours of observation). The temperature was held constant at about 35±2°C by an air stream, and samples were observed with an Axiovert 10 fluorescence microscope (Zeiss, Jena, Germany) equipped with a short arc mercury lamp HBO 100 W/2, a ×63/1.4 NA oil immersion objective, and standard FITC- or TRITC filters. For immunofluorescence pictures were taken with a cooled 12 bit interline CCD-camera under the control of the MetaMorph® software package (both from Visitron, Puchheim, Germany), and printed as 8 bit-depth images with a digital color printer (Fujix NC-500, Fujifilm, Tokyo, Japan). For quantifying tau's expression level, images were acquired under identical conditions (exposure time: 0.2 seconds, image depth: 16 bit, image size: 1280×1024 pixels). The digital images of individual cells had been processed by background subtraction and shadowing-correction algorithms before gray levels of the fluorescent signals were measured via the threshold function of the software. For real time experiments, time series were also captured under identical

conditions (duration: 120 seconds, time interval: 1 second (dead time: 50 milliseconds), exposure time: 0.5 second, image depth: 8 bit, image size: 640×512 pixels, 2×2 vertical and horizontal pixel binning to accelerate digital data acquisition). The resulting image stack of about 40 Mbyte was stored on a local computer.

Data analysis

A macro routine of the software was used to track individual particles interactively. In the case of GFP-VSVG stained cells, we took the center of the fluorescent Golgi area as a reference and interpreted all vesicles (diameter ~30-300 nm) that were transported radially towards the cell periphery as plus-end directed and those that moved into the cell center as minus-end directed. Vesicles transported tangentially were not scored. The classification is based on the fact that the vast majority of MTs are oriented with their plus-ends towards the periphery and the minus-ends anchored at the MTOC near the nucleus and the Golgi apparatus. In CHO cells, some MTs are not radially oriented because of looping. To ensure that the interpretation 'outbound movement = plus-end directed and inbound movement = minus-end directed' was correct, motility parameters were also measured after the MT organization was randomized by treating the cells with nocodazole/taxotere (see above). The observation time of individual particles varied from 20 seconds to 120 seconds (mean ~50 seconds) depending on how long individual particles stayed within the focal plane. In order to subtract the contribution from random Brownian motions we only analyzed vesicles that moved ≥1 μm, and a vesicle was considered as actively transported if its velocity was ≥0.3 μm/second. The following parameters were measured: velocity v (μm/second); distance of transport flanked by resting states (run length L, μm); reversal time = interval between movement in one direction and reversal in the opposite direction, i.e. $t_{+/-}$ is the time between the beginning of an outbound run until the turnaround towards the cell center (including intervening resting periods), $t_{-/+}$ indicates the opposite. Reversal frequencies $f_{+/-}$ or $f_{-/+}$ (second^{-1}) are the reciprocals of the reversal times. Furthermore we analyzed the ratio of plus-end and minus-end transported vesicles (flux ratio R = n_+/n_-) within a constant time period of 120 seconds and an area of 50 μm^2 randomly placed in 3-5 different regions per cell. For the determination of the flux ratio of mitochondria the total cell area was analyzed. Otherwise, basically the same procedures were carried out for motion analysis of mitochondria, with the exception that reversal frequencies of the individual organelles were not measured because of their rare occurrence. Alternatively, the fraction of mitochondria moving in the plus or minus directions was analyzed. Only those mitochondria were considered as actively transported which were translocated ≥1 μm and moved faster than 0.3 μm/second. In contrast to the exocytotic vesicles, the majority of the mitochondria could be observed during the entire observation time of 2 minutes because of their larger size (≥0.5 μm). Finally, we measured the mitochondria and the intermediate filaments-containing area of fixed cells relative to their total size. The data were obtained from parallel experiments with cells that showed similar expression levels of the tau protein.

RESULTS

The experiments described here were designed to determine how tau protein and its subdomains affect vesicle and organelle movement in a cellular environment. We selected CHO cells because they do not normally express tau so that any observable effects should be solely due to the exogenous protein. Besides easy handling, CHO cells are well suited for studying transport because of their flattened form and their size which facilitates observation and microinjection. To monitor the effects of tau'second projection- and MT-binding domains,

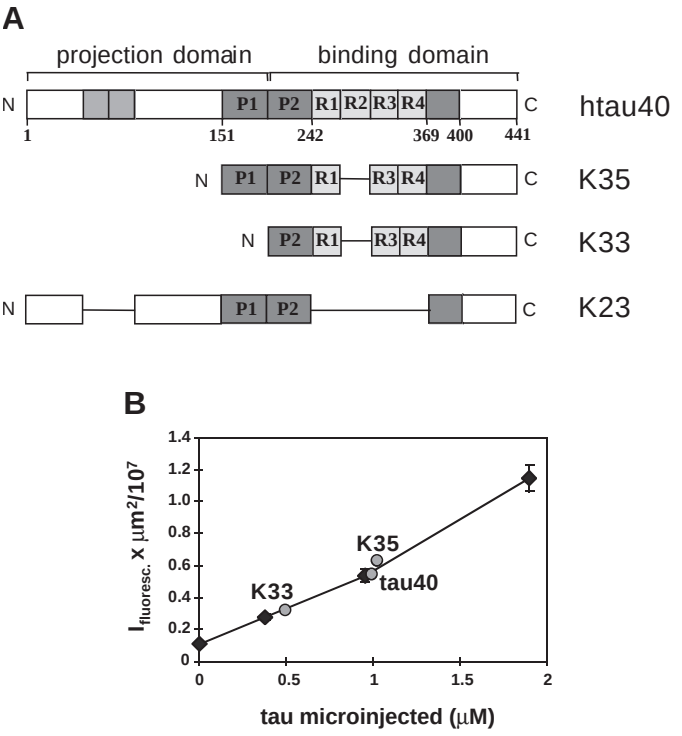

Fig. 1. (A) Domain structure of tau40 and truncated constructs. Tau40 is the longest tau isoform in the human CNS, occurring mostly in axons (Goedert et al., 1989). It consists of 441 amino acid residues and can be divided into an N-terminal projection domain and a C-terminal microtubule binding domain containing 3 or 4 imperfect repeats (R1 to R4, light grey) and basic proline-rich sequences on either side which act as microtubule targeting domains (dark grey). The shaded N-terminal inserts and repeat 2 can be alternatively spliced, resulting in 6 different tau isoforms. The constructs K35, K33 and K23 are derivatives of the embryonic isoform tau23 which contains none of the three inserts. K35 lacks 80% of the projection domain, K33 all of it, and K23 lacks the repeats within the MT-binding domain. (B) Quantification of tau expression in transfected cells. Control cells (mean cell volume: 2.4 pl) microinjected with calibrated quantities of recombinant tau (injected volume: 0.1 pl) were recorded by immunofluorescence and compared with transfected cells. About 160 cells each were measured for the calibration curve (diamonds, mean fluorescent intensity plotted against microinjected tau protein concentration) and for the cells transfected with tau40, K35, and K33 (circles). The tau-concentration for the tau40 and K35-stable cell lines were ~1.0 μM, for the K33-stable cell line ~0.5 μM. Error bars = s.e.m. For data points without an error bar the values range within the symbol size.

cells were stably transfected with the following variants (Fig. 1A): full-length tau (tau40), and truncated constructs K35 or K33 which lack most or all of the N-terminal projection domain. In vitro, these constructs bind with similar affinities to MTs (K_d values for htau40: 1.1 μM, for K35: 1.0 μM, and for K33: 1.5 μM; Gustke et al., 1994). The intracellular concentrations of tau in the stably transfected cells were ~1.0 μM for the tau40 cells, ~1.0 μM for K35 cells and ~0.5 μM for the K33 cells (Fig. 1B). Assuming an intracellular tubulin concentration of about 40 μM (Hiller and Weber, 1978), the tau/tubulin ratio remained in the range of endogenous MAP levels (1:40-1:80; Bulinski and Borisy, 1980; Drubin et al., 1985; Brandt et al., 1995). As shown earlier (Ebneth et al.,

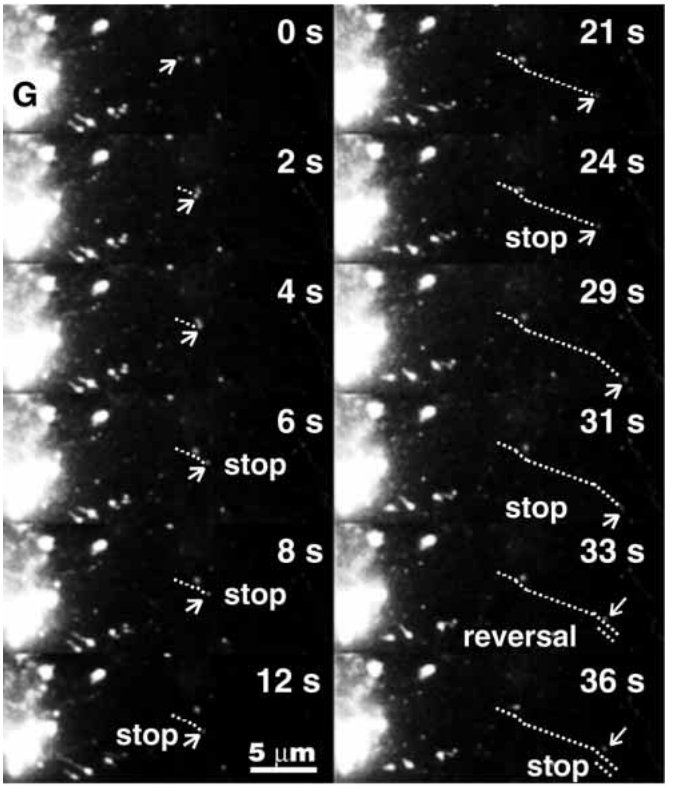

Fig. 2. Real time observation of exocytotic vesicles and their motility. The tau-stable cell lines and the controls were transiently transfected with GFP-VSVG. The time series (intervals as indicated) shows the principal features of the motion of single vesicles observable in living cells. For better illustration a vesicle of ~300 nm in diameter is shown. The vast majority of vesicles analyzed were <100 nm. The vesicle (arrow) moved on average ~0.7 μm/second, had several stops (at 6 seconds, 12 seconds, 24 seconds, 31 seconds, 36 seconds), and changed direction (at 33 seconds). The total distance of translocation was ~12 μm within the 36 seconds of observation time. Note that in general the track pattern (broken line) of vesicle movement is erratic due to reversals which occur stochastically (Wacker et al., 1997). The track shown here illustrates the three characteristics of the motion behavior; i.e. runs, stops and reversals. G, Golgi area stained with GFP-VSVG.

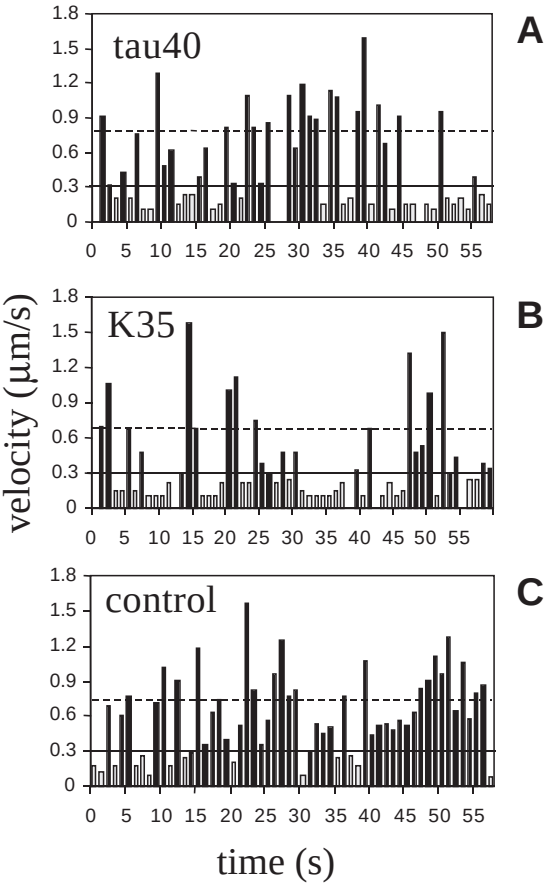

Fig. 3. Discontinuity in the movement of single vesicles illustrated by histograms of speed vs time. Vesicles were considered to be actively transported (irrespective of direction) if their velocities were ≥0.3 μm/second (black columns), and breaks were characterized by values below the threshold of 0.3 μm/second (grey columns). The plots show that on average the motion of the vesicle tracked in the tau-stable cells (tau40 and K35, respectively) was more often interrupted by pauses compared to the vesicle measured in the control (note that there are fewer black bars above threshhold in the transfected cells). By contrast, the mean velocities (broken lines) of all three vesicles measured were similar (tau40: 0.81±0.07 μm/second (*n*=29), K35: 0.66±0.07 μm/second (*n*=24), control: 0.76±0.04 μm/second, s.e.m., *n*=41). Column width is within the interval of one second.

1998) the total concentration of MAPs increases about two to threefold in the tau stable CHO cells; this leads to an overall retardation of kinesin-dependent transport which causes, among others, the clustering of mitochondria around the MTOC.

Tau protein and exocytotic vesicle transport

Exocytotic vesicles were fluorescently labeled by transient expression of GFP-VSVG protein (Urbani and Simoni, 1990; Scales et al., 1997). Their behavior showed the following features (Figs 2, 3): individual vesicles were rapidly transported along random tracks, paused frequently, then continued either in the same direction, changed direction stochastically, or reversed their direction. The time series in Fig. 2 illustrates this behavior. The discontinuity in the movement is analyzed in Fig. 3 by plotting the velocity vs time of typical vesicles in different cells, irrespective of the direction of movement. Using cells stably expressing GFP-tau (which decorated and thus visualized microtubules) and transiently transfected with GFP-VSVG we ascertained that translocation events above the threshold of 0.3 μm/second indeed occurred along MTs (not shown). Both features, rapid transport in all directions and MT dependence point to the contribution of plus-end as well as minus-end directed motors bound to a single vesicle. Since the majority of MTs in CHO cells have a radial orientation where the plus-ends point to the cell periphery and the minus-ends converge at the MTOC near the Golgi apparatus and the nucleus, this system allows one to determine motility parameters separately for plus-end and minus-end directed transport. This was done by grouping the transported vesicles into three directional categories with respect to the localization of the Golgi stain, i.e. inbound (minus-end directed), outbound (plus-end directed), or

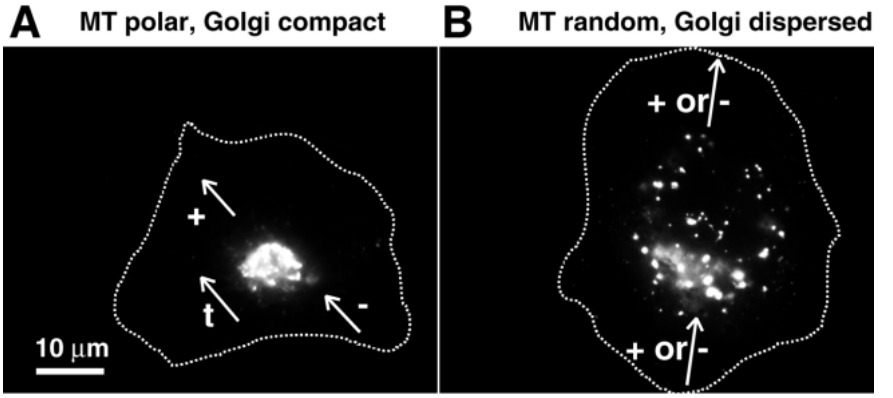

Fig. 4. GFP-VSVG stained Golgi and definitions of vesicle movement. (A) The tau-stable cell lines and the controls were transiently transfected with GFP-VSVG. The green fluorescent stain colocalizes with the Golgi apparatus and with single vesicles (diameter 30-300 nm, Lippincott-Schwartz, 1998). The interpretation of the different directions are indicated by the arrows: (+) plus-end-directed (outbound from Golgi to cell periphery) and (-) minus-end-directed movement (inbound), taking the Golgi stain as the reference which indicates the location of the MTOC and the microtubule minus-ends. (t) denotes vesicles moving 'tangentially' that cannot be classified as plus or minus-end directed. (B) Dispersion of the Golgi elements after randomization of the MT-organization in the cells treated with nocodazole/taxotere. Since the microtubules are no longer centered on the MTOC, inbound or outbound vesicle traffic can not be identified as plus- or minus-end directed. The cell dimensions are indicated by the dotted lines.

tangential to the cell periphery (microtubule polarity uncertain) (Fig. 4).

The average velocity of a moving vesicle was around 1 μm/second (maximum values up to 2.5 μm/second) in both directions. There was no major difference between cells transfected with tau or its microtubule-binding domain (K35) and control cells, suggesting that tau had no influence on the motor activity itself (Fig. 5A). By contrast, run lengths were decreased almost 2-fold, from ~3 μm in the controls to ~1.7 μm in the tau-transfected cells. The decrease was similar for both directions of vesicle movement (Fig. 5B). The result suggests that tau induces more 'stop signs' for the traffic but otherwise leaves the movement itself unaffected. We also conclude that the stop signs do not depend on the projection domain of tau since tau40 and K35 had the same effect.

A different picture emerges for the reversal frequencies (Fig. 5C). For inbound reversals, from the plus to the minus direction, this parameter was not affected by tau ($f_{+/-}$ ~0.12-0.15 second^{-1}). However, outbound reversals (from minus to plus) were about twice as frequent, consistent with the need of secretory vesicles to approach the plasma membrane ($f_{-/+}$ ~0.23 and 0.30 second^{-1} for control and K35, respectively). This higher frequency of outbound reversals was suppressed by full-length tau40 ($f_{-/+}$ ~0.12 second^{-1}). Thus, moving outward appears to be inhibited by tau, in particular by the projection domain. This result was confirmed by another experiment in which we measured the ratio between the number of vesicles leaving or returning to the Golgi area (flux ratio R = n_+/n_-; Fig. 5D, right). This ratio was similar for controls and K35 cells (1.55 and 1.42), showing that ~50% more vesicles leave the Golgi area than returning, consistent with ongoing exocytosis. However, the ratio was significantly lower for cells with full-length tau (0.89), indicating that there was little or no net outbound flux of vesicles. These data argue

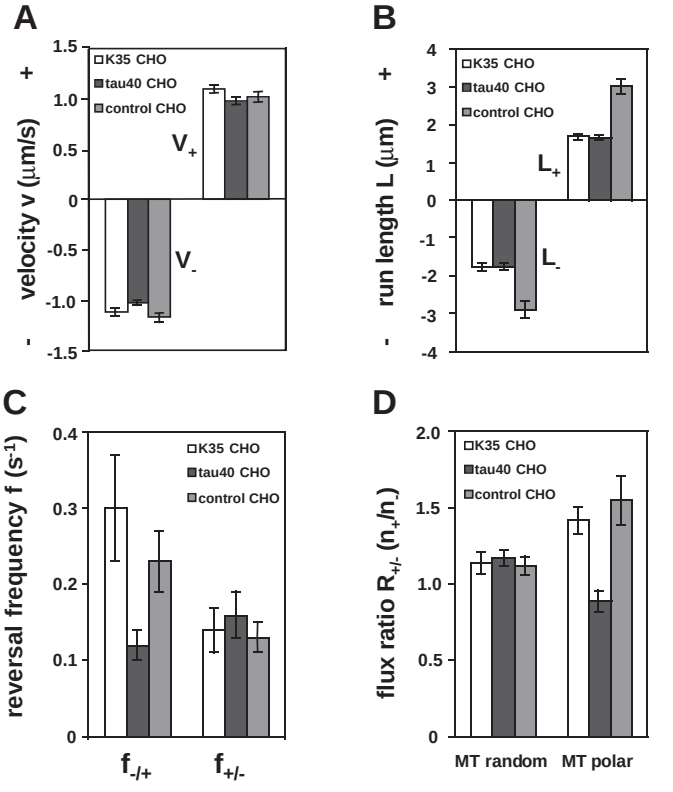

Fig. 5. Quantification of vesicle movement. For data extraction of the parameters of the vesicle transport in A-C about 30 cells were analyzed for each cell line, covering 70-120 single particles (~2-4 per cell). For the determination of the flux ratio (D) about 10 cells for each cell line and 3-5 areas per cell of 50 μm^2 each were analyzed. Error bars represent s.e.m.. Cell lines are as indicated upper right or left (K35, tau40 and control). (A) The velocities of vesicle movement (479-1187 values scored per cell line) were not influenced by tau. (+), plus-end directed; (-), minus-end directed. (B) The run lengths of vesicle movement were significantly decreased in both tau-transfected cell lines and in both directions ($P \leq 2.3\times10^{-8}$, 169-287 values scored per cell line). (C) Reversal frequencies in control cells and K35 cells were higher for outbound reversals ($f_{-/+}$, left group of bars) than for inbound reversals ($f_{+/-}$, right group of bars). But outbound reversals were significantly ($P \leq 0.01$) suppressed by full-length tau (30-48 reversals scored per cell line). (D) Flux ratio R = n_+/n_- of vesicles moving out of vs into the Golgi area (30-50 values scored per cell line). With polar microtubules (right group) the value is ~1.5 for control cells and K35-cells, but not in the presence of tau40 where both fluxes roughly balance each other (R ~0.90, $P \leq 0.0005$). The imbalance of fluxes disappears after randomizing the MT organization (left group, R ~1.1).

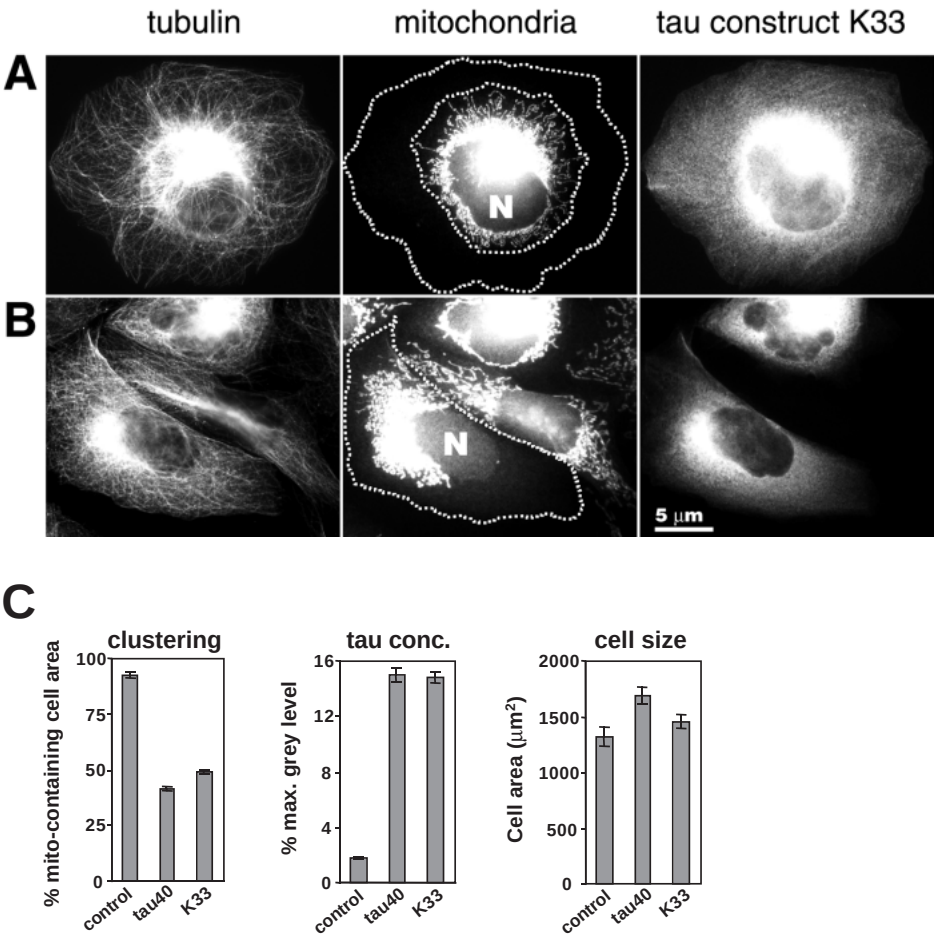

Fig. 6. Perinuclear clustering of mitochondria in CHO cells induced by tau construct K33. Cells were fixed with paraformaldehyde (see Materials and Methods) which tends to dissociate tau from the cellular MTs, but does not extract tau out of the cells (Preuss et al., 1997), and is therefore suitable for quantification of tau expression. (A and B) Two examples of cells with microtubules stained with anti-tubulin antibody DM1A (left panel), mitochondria with MitoTracker™ Red (middle), and HA-tagged tau detected by polyclonal rabbit HA-tag antibody (right panel). The same labeling was performed for quantifying the intracellular distribution of mitochondria (see C). (A) Microtubules show a normal distribution (left), but mitochondria are clustered around the nucleus (N, middle) because minus-end directed transport is predominant in a cell expressing tau-K33. The area containing mitochondria and the cell perimeter are indicated by the broken lines. The expression of HA-tagged K33 is shown on the right. Tau is no longer bound to microtubules as a result of fixation (without fixation, most tau would be bound to microtubules; Olson et al., 1995; Illenberger et al., 1998). (B) Similar example showing three cells, two of which contain tau-K33 (upper and lower), the middle cell does not contain tau. Left: all three cells show a normal microtubule network. Middle: the upper and lower cells show clustered mitochondria at the cell center, the middle cell shows mitochondria dispersed throughout the cell. Right: the upper and lower cell contains tau-K33, the middle one does not. The examples also show that the clustering of mitochondria does not depend on the cell size or form (round or elongated). (C) Quantification of distribution of mitochondria. Right: cells were selected for analysis on the basis of comparable size (apparent area ~1300-1600 µm^2). Middle: only the transfected cells contained HA-tagged tau or K33. Left: the mitochondria-containing area decreased about twofold in the tau-transfected cells. Number of cells measured was about 75 for each cell line. Error bars, s.e.m.

that the outbound flow of secretory vesicles is inhibited by tau and requires the projection domain in addition to the microtubule-binding domain.

Differences in plus-end- and minus-end-directed vesicle transport are leveled out by randomizing the cellular MT organization

If the differences between inbound and outbound traffic were based on a polarized microtubule network they should disappear when the microtubule directions are randomized. This can be achieved by treating the cells first with nocodazole (which disassembles MTs) and subsequently with taxotere (which allows reassembly independently of the MTOC; DeBrabander et al., 1986). One consequence of this treatment is the dispersion of the Golgi material away from the MTOC or even throughout the whole cell (Fig. 4B), consistent with the observation that the minus-end motor dynein ensures proper positioning of the Golgi apparatus near the MTOC (Burkhardt et al., 1997). We analyzed the flux ratio n_+/n_- to check the significance of the imbalanced vesicle trafficking measured for the tau40 CHO cells. Taking the (dispersed) Golgi area as a reference, the ratios R between outbound and inbound vesicles were close to 1 and similar in transfected and control cells (~1.1, Fig. 5D, left), contrary to the higher value when microtubules are polarized (Fig. 5D, right). This demonstrates that any difference between the directions of traffic are due to the polarity of the microtubule tracks, and that an efficient outbound traffic requires radially polarized microtubules.

Tau protein and the mitochondrial transport system

Earlier work (Ebneth et al., 1998) has shown that overexpression of tau induced a perinuclear clustering of mitochondria. This suggests that tau preferentially inhibits the plus-end directed motor (e.g. the mitochondrial kinesin motor Kif5B; Tanaka et al., 1998). Even tau's MT-binding domain alone (construct K33) is sufficient to shrink the mitochondria-containing area towards the MTOC to the same extent as full-length tau (Fig. 6A,B, center): mitochondria occupy ~90% of the area of control cells, but only ~45% in the tau-stable cell lines (Fig. 6C, left). This shows that tau's MT-binding domain is the major determinant in creating the clustered appearance of mitochondria. Note that this is in contrast to the case of the exocytotic vesicles described above where the microtubule-

binding domain of tau equally affects plus- and minus-end directed transport by decreasing the run lengths of the moving organelles and causes no pronounced clustering near the cell center (presumably because of their higher overall mobility). In the case of vesicles, only full-length tau was able to shift the equilibrium of bidirectional transport towards the minus-ends as monitored by the decrease of the flux ratio R = n_+/n_- (Fig. 5D).

We therefore asked which of the motility parameters would be affected by tau in the mitochondrial transport system. Before the tau-stable cells could be analyzed the mitochondria had to be dispersed (to avoid their overlap by the clustering effect). This was achieved by disassembling microtubules with nocodazol, followed by removal of the drug to allow the reconstitution of a polarized microtubule network centered at the MTOC; the movement of mitochondria was then observed within ~1 hour, long before they were clustered again at the MTOC (~5 hours; Fig. 7). The particles did not show significant changes in speed in the tau-stable cell lines, compared to controls (average ~0.6 μm/second, with maximum values up to 1.8 μm/second; Fig. 8A); this is similar to the results with secretory vesicles (Fig. 5A). The run lengths of mitochondria transport showed a pronounced decrease in the tau-stable cell lines by ~30-40% of control (from ~1.5 to ~1.0 μm; Fig. 8B), both in plus-end and minus-end direction; this is again comparable to the data of secretory vesicles (Fig. 5B). This means that with regard to speed and run length, the MT-binding domain of tau acts in a similar fashion on the transport of mitochondria and of exocytotic vesicles. Secondly, we conclude that neither speed nor run length are the transport parameters that can account for the clustering of mitochondria near the MTOC (Fig. 6).

Because velocities and run lengths were not differentially affected by tau in the plus or minus direction, we additionally measured the fraction of actively transported organelles, compared to their total number. This parameter reflects the successful attachment of the motors on the MTs (somewhat analogous to the reversal frequency described above, except that in the case of mitochondria reversals are too rare to be scored reliably). A translocation event was scored only when a particle moved more than 1 μm and faster than 0.3 μm/second, irrespective of the direction. By this criterium, control cells showed 4-5% of the organelles moving within 2 minutes of observation (Fig. 8C, left). This value dropped two- to threefold in the tau40-stable cell lines (~1.5-2%). When the translocation events were grouped according to direction, we found that tau40 or K35 decreased the fraction of plus-end directed movements about 10-fold (from ~1.8% to 0.2%, Fig. 8C). By contrast, the population that moved in the minus-end direction were decreased only by ~1.3-fold (from ~1.6% to 0.9-1.2%). The differences observed were leveled out in cells in which the MT organization had been randomized by nocodazole/taxotere treatment (Fig. 8C, columns labeled *htau40). This argues for the significance of the observed differences, even though the total fraction of moving mitochondria was small. Even construct K33 (= microtubule-binding domain only), which showed a lower expression level than K35 or tau40 (Fig. 1B), generated a clear differential impairment of the plus-end and minus-end directed transport of mitochondria: we observed no change of the minus-end directed transport, but a fourfold decrease in the plus-end directed transport, compared to the control (from ~1.6% to 0.4%). Thus, tau preferentially reduces the fraction of mitochondria actively transported in plus-end direction (decrease of the flux ratio R = n_+/n_- from 1.1 to 0.2, Fig. 8D). This effect accounts for the observed phenomenon of perinuclear clustering.

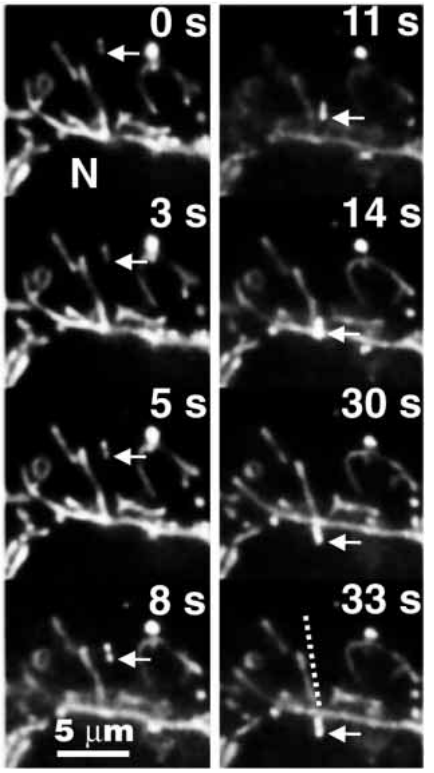

Fig. 7. Real time observation of single mitochondria in CHO cells. Tau-stable cells were treated with nocodazole for 1 hour to dissolve the cluster of the mitochondria around the MTOC and allow their dispersion. The drug was removed by washing in order to enable the reconstitution of a microtubule network centered on the MTOC. Cells were stained for mitochondria (MitoTracker™ Red, final concentration: 200 nM, incubation: 10 minutes) and observed by time-lapse microscopy. The time series (33 seconds out of 2 minutes of total observation time, intervals as indicated upper right) of an enlarged detail shows a mitochondrion (arrow, length ~1.5 μm, appearing as two dots) that is actively transported towards the nucleus N (velocity above threshold of 0.3 μm/second) but interrupted by pauses (where v < 0.3 μm/second, at 5 seconds-8 seconds and 33 seconds). The velocity of active motion above the threshold was ~0.5 μm/second and the total distance of translocation within the total time of observation (2 minutes) was 6.6 μm (broken line; effective velocity only 0.06 μm/second). Note that only a minority of mitochondria show movement. For the tau40-stable cell line, the total displacement of those mitochondria showing movement was 3.47±0.35 μm per 2 minute interval (n=24) for plus-end directed transport, and 4.38±0.30 μm per 2 minute (n=59) for minus-end directed transport.

The MT-binding domain overexpressed in CHO cells causes a perinuclear clustering of the vimentin intermediate filaments

The results presented so far demonstrate that tau's MT-binding domain can interfere with MT/motor-protein dependent

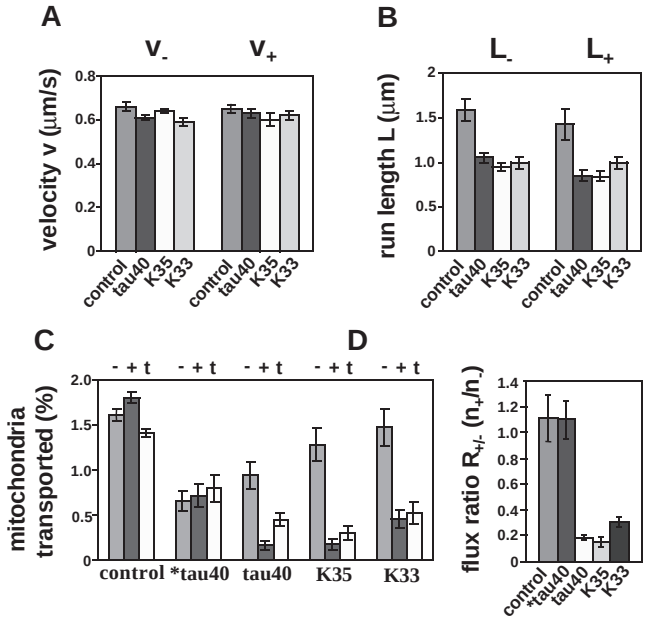

Fig. 8. Quantification of mitochondria movement. (A and B) 20-30 cells and 24-59 single particles each of the different cell lines were tracked. (C and D) 40-50 cells were analyzed for each of the cell lines. The total number of mitochondria per cell ranged between 100-700. Error bars indicate s.e.m. (+), plus end directed, (–), minus end directed. (A) The velocities were similar in the plus and minus direction and did not depend on tau (127-448 values scored). (B) The run lengths in the tau-stable cell lines decreased by ~30-40% of control ($P \leq 0.03$), in both directions. (100-326 run lengths scored). (C) The fraction of moving mitochondria was subdivided by direction, taking the nucleus as the reference (t, tangential; +, plus-end directed; –, minus-end directed). In tau-stable cells there is a general decrease in motile mitochondria. This is particularly pronounced for plus-end directed movement, but less prominent for minus-end directed movements. In tau40 cells with randomized MT networks (*tau40) the differences between plus-end and minus-end directed transport of mitochondria disappeared. (D) The flux ratio R between outbound and inbound transport of mitochondria was about 1 in control cells. It drops ~4-5-fold in cells expressing tau, showing that outbound movement is impaired.

intracellular transport. To corroborate whether this is a general property of tau we also studied the distribution of intermediate filaments (IFs) which are spread out along the MTs powered by kinesin (Gyoeva and Gelfand, 1991; Yoon et al., 1998). IF-spreading was determined by measuring the apparent extent of the IF-containing cell area of fixed and anti-vimentin stained cells (Fig. 9A). This area is reduced about 3-fold, from ~75% in control cells to ~25% in cells expressing tau (Fig. 9B, left). Full length tau and the constructs had similar effects, arguing that it was based mainly on the MT-binding domain of tau.

Weakly binding tau constructs do not affect MT-dependent intracellular transport

As an additional control we tested a tau construct which lacks the repeats within the MT-binding domain and therefore binds with lower affinity to MTs (K23, Fig. 1A, K_d = 7 μM; Gustke et al., 1994). This tau variant did not induce clustering of the intermediate filaments in CHO cells transiently transfected with the HA-tagged K23, even at higher expression levels (Fig. 10). Likewise, a wild-type distribution of mitochondria was observed in the K23-stable cell line (see Fig. 3e,f, in Ebneth et al., 1998). The run lengths of the GFP-VSVG-stained vesicles in this cell line showed no changes compared to the mock-transfected cells (L_+ = 2.8±0.2 μm, s.e.m., n=234; $L_–$ = 2.9±0.3 μm, s.e.m., n=198; compare with Fig. 5B). This argues that tau is directly responsible for the phenotypes investigated, and that tight binding to microtubules is required. Thus, tau's MT-binding domain can influence the transport of very different intracellular cargoes by affecting mainly the plus-end directed transport mediated by kinesin-like motor proteins.

DISCUSSION

In this study we have analyzed how tau protein affects the microtubule-based motility of single particles in cells. The work was triggered by earlier observations that tau caused the accumulation of mitochondria near the MTOC, retraction of the endoplasmic reticulum, and slow-down of exocytosis. These events could be interpreted in terms of a retardation of plus-end directed transport along microtubules mediated by kinesin, compared to that of minus-end directed transport by dynein (Ebneth et al., 1998). We therefore wanted to ask how tau exerted its influence on the level of single particles, and which parameters of motility were affected, e.g. velocity, run length, fraction of motile particles, etc. We compared tau protein constructs of different sizes, and tested the motility of three different intracellular structures, exocytotic vesicles, mitochondria, and intermediate filaments, all of which are known to move along microtubules. Vesicles and mitochondria are linked to the motors via membrane/organelle bound adaptor-proteins, such as kinectin or dynactin (Kumar et al., 1995; Burkhardt et al., 1997), complexed with membrane-matrix components like spectrin or ankyrin (Lippincott-Schwartz, 1998), vimentin IFs and MTs may be crosslinked directly via kinesin (Liao and Gundersen, 1998). Exocytotic vesicles and mitochondria can be translocated along MTs towards their plus- and minus-ends by kinesin or cytoplasmic dynein (Brady, 1995; Vallee and Sheetz, 1996; Khodjakov et al., 1998). By contrast, intermediate filaments or their precursors can be transported only towards the cell periphery by kinesin (Gyoeva and Gelfand, 1991; Prahlad et al., 1998), whereas the opposite transport more likely depends on actin microfilaments (Hollenbeck et al., 1989).

The main results of the motion analysis can be summarized as follows: at first sight, vesicles appear to show a largely random pattern of motion since their association with microtubles is only transient, interrupted by breaks, reversals, and directional changes, and since this is superimposed on a background of Brownian motion (Figs 2, 3; cf. Wacker et al., 1997). The random processes can be largely eliminated by applying a threshold, such that only movements faster than 0.3 μm/second and longer than 1 μm are considered as active transport. With this constraint, it becomes apparent that vesicles move about equally fast towards the plus end of microtubules (outbound towards the cell periphery) and to the minus end (inbound towards the Golgi/MTOC), at ~1 μm/second (Fig. 5A). These velocities are broadly consistent with the speeds of kinesin or dynein observed in vitro and with the speeds of particles in fast axonal transport (Hirokawa,

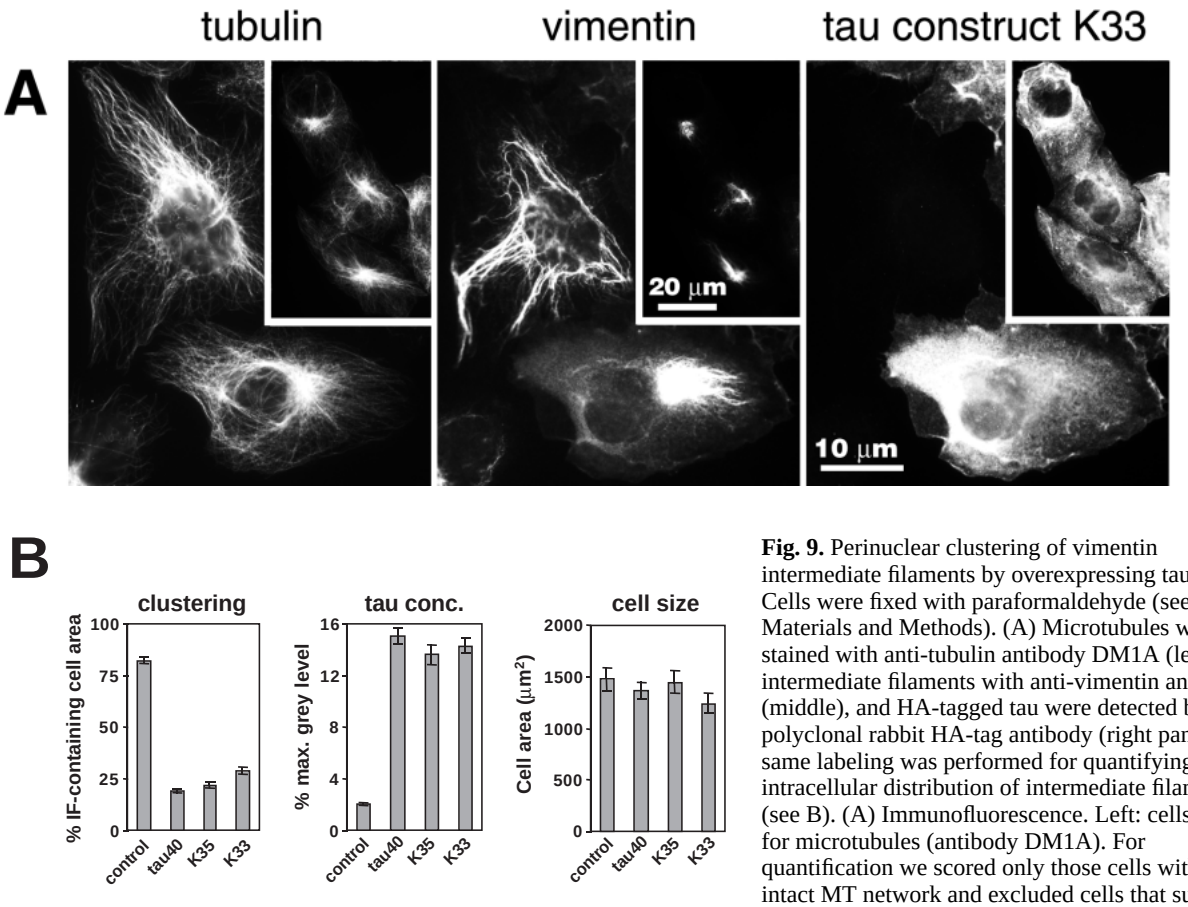

Fig. 9. Perinuclear clustering of vimentin intermediate filaments by overexpressing tau protein. Cells were fixed with paraformaldehyde (see Materials and Methods). (A) Microtubules were stained with anti-tubulin antibody DM1A (left panel), intermediate filaments with anti-vimentin antibody (middle), and HA-tagged tau were detected by polyclonal rabbit HA-tag antibody (right panel). The same labeling was performed for quantifying the intracellular distribution of intermediate filaments (see B). (A) Immunofluorescence. Left: cells stained for microtubules (antibody DM1A). For quantification we scored only those cells with an intact MT network and excluded cells that suffered from fixation or other damage. Middle: staining by anti-vimentin antibody. There is a pronounced clustering of vimentin near the cell center due to the presence of tau (cell at bottom). This clustering is not observed in the cell at the center which does not express tau and therefore shows a well-spread vimentin intermediate filament network. The background fluorescence stems from the strong TRITC-signal of the tau stain that partly passes the FITC-filter. Right: tau-K33 is expressed only in the bottom cell, but not in the middle cell. The insets show that the clustering of vimentin (middle) is a prominent feature of cells with an intact MT network (left) expressing the tau construct K33 (right). (B) Quantification of IF-clustering. By analyzing the tau-stable cells of equivalent size (histogram on the right, ~1500 μm^2) and with similar anti-HA immunofluorescent stain (in the middle), the IF-containing area decreased three- to fourfold (on the left). All tau constructs had similar effects. Number of cells measured was about 70 for each cell line. Error bars, s.e.m.

1998; Ratner et al., 1998). Furthermore, the run lengths of vesicles are the same in both directions, ~3 μm (Fig. 5B). How, then, does a secretory vesicle reach its destination at the plasma membrane? Part of the answer is statistical: if a vesicle meets the plasma membrane it is exocytosed, independently of how it arrived there (Rothman, 1994). This is one reason why many cells continue functioning almost normally even when the microtubules are temporarily disrupted, e.g. by nocodazol. However, in addition the microtubule network, centered on the MTOC and polarized towards the periphery, provides a directional bias. This is best seen from the reversal frequencies and the net fluxes. A vesicle moving in the 'wrong' direction (inbound) will be kicked back towards the periphery much more frequently than a vesicle already moving in the proper direction (Fig. 5C). This property is reflected in the flux ratio; the number of vesicles moving outbound, away from the Golgi area, is 50% larger than those moving inbound (Fig. 5D).

How does tau affect these transport parameters of exocytotic vesicles? Surprisingly, tau has no influence on speed at all, showing that once a vesicle is on its track, neither kinesin nor dynein motors shift gears because of tau molecules that might be in the way (Fig. 5A). However, tau does reduce the run length almost 2-fold, from 3 to 1.7 μm (Fig. 5B). By assuming a homogeneous distribution of tau on the MTs, a tau/tubulin ratio of ~1:40 (Fig. 1B), and movement of motors along single MT protofilaments, a tau molecule would occur along a protofilament every ~0.32 μm. Thus a run length of 1.7 μm would correspond to ~6 encounters between a motor and a tau molecule. The decrease in run length argues that the chance of a motor slipping and losing its track rises with the number of MAPs on the microtubules. In kinetic terms, it appears that tau does not affect the k_{cat} of the motors but reduces the apparent processivity, possibly by perturbing the cross-talk between the moving motor heads when an encounter occurs. It is again surprising that these changes occur equally for both directions, and they require only tau's microtubule-binding domain, not the projection domain, so that steric hindrance effects are not important in this context (Fig. 5B); however, steric hindrance effects might become more important with MAPs having larger projection domains, such as MAP2 and MAP4 which also affect vesicle motility (Sato-Harada et al., 1996; Bulinski et al., 1997).

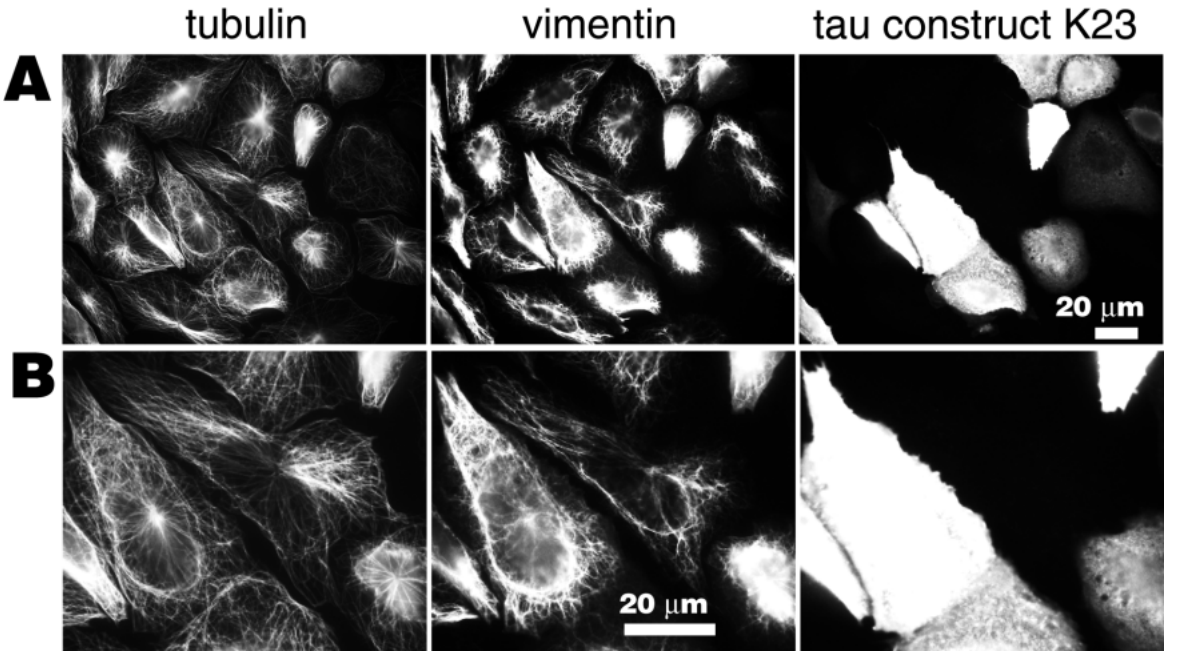

Fig. 10. The weakly binding tau construct K23 does not induce the clustering of vimentin intermediate filaments. Cells were transiently transfected with HA-tagged K23 and fixed with paraformaldehyde (see Materials and Methods). (A) Microtubules were stained with anti-tubulin antibody DM1A (left), intermediate filaments with anti-vimentin antibody (middle), and HA-tagged tau was detected by polyclonal rabbit HA-tag antibody (right), (B) represents an enlargement of the two cells at the center in A. Even in cells with high expression levels of the HA-tagged construct K23 (e.g. the cell in the middle in A and on the left in B), the IF network is well spread throughout the cells (see the vimentin stain in the middle of A and B, which covers almost 100% of the total cell area). For quantification we scored only cells with an intact MT network and excluded cells that suffered from fixation or other damage (for example, the cell on the upper right in A shows a less dense MT network (left), the vimentin stain covers ~50% of the total cell area (middle), but the expression level of K23 in this cell is low (right). The IF-containing cell area was 70.3±5.1% (s.e.m., *n*=52) for the K23-transfected cells and 75.6±4.7% (s.e.m., *n*=67) for the controls.

The most sensitive parameters for directionality are the reversal frequencies and flux ratios. While inbound reversals are not affected by tau, there is a strong reduction of outbound reversals by tau40. In other words, the cell's ability to kick a vesicle back onto its outbound track is impaired. The reasons are not known, but it could be explained, for example, by an inhibition of kinesin attachment after the release of dynein from the microtubule. Similarly, the flux ratio is ~1.5 in control cells, consistent with a predominance of outbound traffic, but it drops to ~1 in the presence of tau40 so that there is no net outbound flux. In these cases, we also find a clear requirement for tau's projection domain: constructs like K35 which lack this domain do not have an appreciable effect, even though they bind tightly to microtubules (Gustke et al., 1994).

In the case of mitochondria the effects of tau on short-term movements are less apparent because only a small fraction (<5% of mitochondria) show any movement at all over a 2 minute interval. Nevertheless, from our earlier experiments we knew that there must be long-term effects of tau which allows minus-end-directed transport to dominate, so that mitochondria accumulate near the MTOC. For the small fraction of particles moving at any time we conclude that the effects on velocity and run length are similar to those observed with vesicles, i.e. the velocity is the same in both directions (~0.6 μm/second, Fig. 8A) and is not affected by tau at all, the run lengths are the same in both directions (~1.5 μm), and they are diminished about 1.7-fold by tau, irrespective of its domain composition. It is in fact

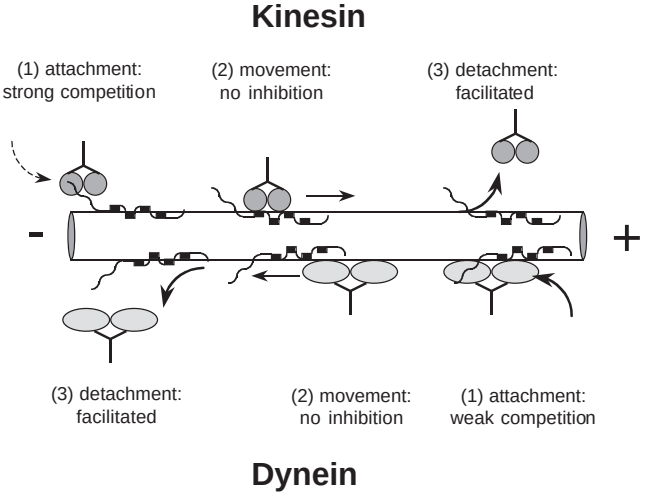

Fig. 11. The attachment/detachment cycle of MT-based organelle transport is affected by tau, but not the speed. Tau or endogenous MAPs are shown as hooks bound to a microtubule. A vesicle with its attached motor complex must attach to a microtubule, move along, and detach. The velocity is not altered by tau. Vesicles detach more readily when the number of tau molecules is increased; this leads to shorter run lengths in both directions, both for kinesin and dynein. The initial attachment becomes more difficult with increasing tau. This inhibition is more pronounced for kinesin than for dynein so that minus-end directed movements become more dominant.

remarkable that mitochondria, despite their much larger size, show speeds and run lengths that are rather comparable to those of vesicles (only ~2-fold lower), confirming again that motors, once at work, move at (nearly) their intrinsic speed (much like an icebreaker in thin ice). Given these similarities, we would anticipate that the reversal frequencies would be more sensitive parameters for directionality and tau-dependence, but these could not be measured reliably because of their rare occurrence. However, the bias on movement induced by tau becomes apparent if we group the moving particles according to direction: this shows that plus-end directed movements are much more severely impaired (up to 10-fold) than minus-end movements (Fig. 8C). Similarly, the flux ratio for outbound vs. inbound flux in normal cells is ~1 (Fig. 8D), indicating a balance between plus-end and minus-end directed motion (as expected for mitochondria which are not secreted). This parameter is reduced ~5-fold by tau which explains the gradual clustering of mitochondria at the MTOC. We also note that all tau forms are about equally potent, even in the K33-transfected cells where the concentration of expressed protein is lower than for K35 and tau40. Thus, the projection domain of tau is not of primary importance in these conditions. The motion parameters of mitochondria described here are in good agreement with the time of clustering measured by analyzing the mitochondria-containing area of fixed cells (4-5 hours, Ebneth et al., 1998). For example, assuming a cell diameter of ~40 μm on average (e.g. Fig. 6C), each of the mitochondria has to move about 5 μm towards the cell center in order to create the clustered phenotype (mitochondria-containing area = 50% of total cell area). Given the percentages of the organelles transported radially and towards the cell center (0.16% and 0.94%, respectively, Fig. 8C) and the corresponding total translocations per 2 minutes interval of observation (3.5 μm and 4.4 μm, respectively, Fig. 7), the time necessary for reclustering was calculated to be 4.7 hours. This shows that clustering of mitochondria at the MTOC is based on active, fast transport of individual organelles even though the whole process itself is slow.

Finally, we checked the influence of the different tau constructs on the behavior of intermediate filaments which are transported along microtubules in the plus-end direction (Gyoeva and Gelfand, 1991; Prahlad et al., 1998; Liao and Gundersen, 1998). Although we did not visualize individual IF precursor particles, the distribution of the IF network in tau-expressing cells was very reminiscent of that of mitochondria, i.e. the spreading towards the periphery was impaired, and the network appeared to contract towards the cell center (Fig. 9). Here, too, there was no influence of tau's projection domain on the outbound traffic of the IFs. This argues that the effects of tau on kinesin-dependent transport are rather general and make use of similar principles.

It might be argued that the perturbation of transport could be due to indirect effects like cloning artifacts and exogenous gene expression, inhibition of kinesin independently of tau's binding to microtubules, or kinase/phosphatase activities imbalanced in cells overloaded with the phosphoprotein tau. We believe these possibilities can be ruled out for the following reasons: (1) the same phenotypes are observed in three different tau-stable cell lines (tau40, K35, K33). (2) CHO cells transfected with the tau variant K23 that lacks the repeats within the MT binding domain, binds weakly to MTs (K_d = 7 μM, Gustke et al., 1994), yet retains most of the phosphorylation sites for different kinases (Drewes et al., 1997; Illenberger et al., 1998), showed the normal IF-distribution (Fig. 10), did not induce the clustering of mitochondria (Ebneth et al., 1998), and had no influence on the run lengths of the exocytotic vesicles. This provides strong evidence for a direct effect of tau on the phenotypes investigated. However, the exact molecular basis of the interplay between microtubules, motors and tau remains to be established. An attractive hypothesis to explain the different effects of tau on kinesin and dynein would be their distinct modes of walking along a microtubule. While kinesin moves strictly along protofilaments (Kamimura and Mandelkow, 1992), dynein tends to tumble across the microtubule surface (Wang et al., 1995). This feature might give dynein a better chance to bypass tau bound on the MT and find neighboring MT-binding sites free of tau that might facilitate the initial attachment. By contrast, the MT/kinesin attachment complex might represent a complex with more structural constraints that impede its formation in the presence of tau on the MT surface.

In summary, we have analyzed the motions of single particles in cells as a step towards understanding their dependence on microtubules, motors, and MAPs. Secretory vesicles show a strong random component due to Brownian movement, a majority of them is constantly on the move (>60%), and there is a gradual outbound transport bias due to exocytosis. By contrast, mitochondria are largely static (only <5% are seen moving within a 2 minute interval), and they show no outbound bias once they are dispersed in the cell. In spite of these differences, the interplay between microtubules, motors and tau (as a representative MAP) is remarkably similar. Motors, once on a microtubule track, are not perturbed by tau in their instantaneous action (the velocity does not change). However, in the aqueous environment of the cell there is a chance of slipping off the track, and this probability increases with tau (run lengths become shorter, but equally in both directions). The directional bias induced by tau takes place in a very subtle form: the numbers of particles moving in the plus direction decrease more than in the minus direction, and reversals to an outbound path become preferentially reduced. A unifying hypothesis linking these features is that tau impairs the initial approach of plus-end directed motors (i.e. kinesin) onto the microtubule more than that of minus-end motors (dynein), without affecting the actual motion, and without causing a bias in the detachment. This assumption is illustrated in the diagram of Fig. 11. The molecular basis of this biased attachment remains to be established. A simple view, consistent with the reported overlap between MAP and motor binding sites on microtubules (Paschal et al., 1989; Hagiwara et al., 1994) would be that tau blocks the kinesin binding site more efficiently than that of dynein.

We thank I. Thielke and K. Alms for excellent technical assistance. We gratefully acknowledge the generous gift of the GFP-VSVG vector from Th. Kreis and S. Scales (Geneva, Switzerland). This project was supported by the Deutsche Forschungsgemeinschaft.

REFERENCES

Barlow, S., Gonzalez-Garay, M. L., West, R. R., Olmsted, J. B. and Cabral, F. (1994). Stable expression of heterologous microtubule-associated

proteins (MAPs) in chinese-hamster ovary cells – evidence for differing roles of MAPs in microtubule organization. *J. Cell Biol.* **126**, 1017-1029.

Binder, L. I., Frankfurter, A. and Rebhun, L. (1985). The distribution of tau in the mammalian central nervous system. *J. Cell Biol.* **101**, 1371-1378.

Blocker A., Griffiths G., Olivo J. C., Hyman A. A. and Severin F. F. (1998). A role for microtubule dynamics in phagosome movement. *J. Cell Sci.* **111**, 303-312.

Brady, S. T. (1995). Biochemical and functional diversity of microtubule motors in the nervous system. *Curr. Opin. Neurobiol.* **5**, 551-558.

Brandt, R., Leger, J. and Lee, G. (1995). Interaction of tau with the neural plasma-membrane mediated by tau amino-terminal projection domain. *J. Cell Biol.* **131**, 1327-1340.

Bulinski, J. C. and Borisy, G. G. (1980). Immunofluorescence localization of HeLa cell microtubule-associated proteins on microtubules in vitro and in vivo. *J. Cell Biol.* **87**, 792-801.

Bulinski, J. C., McGraw, T. E., Gruber, D., Nguyen, H.-L. and Sheetz, M. P. (1997). Overexpression of MAP4 inhibits organelle motility and trafficking in vivo. *J. Cell Sci.* **110**, 3055-3064.

Burkhardt, J. K., Echeverri, C. J., Nilsson, T. and Vallee, R. B. (1997). Overexpression of the dynamitin (p50) subunit of the dynactin complex disrupts dynein-dependent maintenance of membrane organelle distribution. *J. Cell Biol.* **139**, 469-484.

Chapin, S. J. and Bulinski, J. C. (1991). Non-neuronal 210 kD Mr microtubule-associated protein (MAP4) contains a domain homologous to the microtubule-binding domains of neuronal MAP2 and tau. *J. Cell Sci.* **98**, 27-36.

Chen, J., Kanai, Y. and Hirokawa, N. (1992). Projection domains of MAP2 and tau determine spacings between microtubules in dendrites and axons. *Nature* **360**, 674-677.

DeBrabander,M., Geuens,G., Nuydens,R., Willebrords,R., Aerts,F. and DeMey, J. (1986). Microtubule dynamics during the cell cycle: the effects of taxol and nocodazole on the microtubule system of PtK_2 cells at different stages of the mitotic cycle. *Int. Rev. Cytol.* **101**, 215-274.

Drewes, G., Ebneth, A., Preuss, U., Mandelkow, E.-M. and Mandelkow, E. (1997). MARK, a novel family of protein kinases that phosphorylate microtubule-associated proteins and trigger microtubule disruption. *Cell* **89**, 297-308.

Drubin, D. G., Feinstein, S. C., Shooter, E. M. and Kirschner, M. W. (1985). Nerve growth factor-induced neurite outgrowth in PC12 cells involves the coordinate induction of microtubule assembly and assembly-promoting factors. *J. Cell Biol.* **101**, 1799-1807.

Drubin, D. G. and Nelson, W. J. (1996). Origins of cell polarity. *Cell* **84**, 335-344.

Ebneth, A., Godemann, R., Stamer, K., Illenberger, S., Trinczek, B., Mandelkow, E.-M. and Mandelkow, E. (1998). Overexpression of tau protein inhibits kinesin-dependent trafficking of vesicles, mitochondria, and endoplasmic reticulum: implication for Alzheimer's disease. *J. Cell Biol.* **143**, 777-794.

Feiguin, F., Ferreira, A., Kosik, K. S. and Caceres, A. (1994). Kinesin-mediated organelle translocation revealed by specific cellular manipulations. *J. Cell Biol.* **127**, 1021-1039.

Field J., Nikawa J., Broek D., MacDonald B., Rodgers L., Wilson I. A., Lerner R. A. and Wigler M. (1988). Purification of a RAS-responsive adenylyl cyclase complex from Saccharomyces cerevisiae by use of an epitope addition method. *Mol. Cell Biol.* **8**, 2159-2165.

Goedert, M., Spillantini, M. G., Potier, M. C., Ulrich, J. and Crowther, R. A. (1989). Cloning and sequencing of the cDNA encoding an isoform of microtubule-associated protein tau containing four tandem repeats: differential expression of tau protein mRNAs in human brain. *EMBO J.* **8**, 393-399.

Goodson, H. V., Valetti, C. and Kreis, T. E. (1997). Motors and membrane traffic. *Curr. Opin. Cell Biol.* **9**, 18-28.

Gustke, N., Trinczek, B., Biernat, J., Mandelkow, E.-M. and Mandelkow, E. (1994). Domains of tau protein and interactions with microtubules. *Biochemistry* **33**, 9511-9522.

Gyoeva, F. K. and Gelfand, V. I. (1991). Coalignment of vimentin intermediate filaments with microtubules depends on kinesin. *Nature* **353**, 445-448.

Hamm-Alvarez, S. F., Kim, P. Y. and Sheetz, M. P. (1993). Regulation of vesicle transport in CV-1 cells and extracts. *J. Cell Sci.* **106**, 955-966.

Hagiwara, H., Yorifuji, H., Sato-Yoshitake, R. and Hirokawa, N. (1994). Competition between motor molecules (kinesin and cytoplasmic dynein) and fibrous microtubule-associated proteins in binding to microtubules. *J. Biol. Chem.* **269**, 3581-3589.

Hiller, G. and Weber, K. (1978). Radioimmunoassay for tubulin: a quantitative comparison of the tubulin content of different established tissue culture cells and tissues. *Cell* **14**, 795-804.

Hirokawa, N. (1994). Microtubule-organization and dynamics dependent on microtubule-associated proteins. *Curr. Opin. Cell Biol.* **6**, 74-81.

Hirokawa, N. (1998). Kinesin and dynein superfamily proteins and the mechanism of organelle transport. *Science* **279**, 519-526.

Hollenbeck P. J., Bershadsky A. D., Pletjushkina O. Y., Tint I. S. and Vasiliev J. M. (1989). Intermediate filament collapse is an ATP-dependent and actin-dependent process. *J. Cell Sci.* **92**, 621-631.

Hollenbeck, P. and Swanson, J. (1990). Radial extension of macrophage tubular lysosomes supported by kinesin. *Nature* **346**, 864-866.

Hyman A. and Karsenti E. (1996). Morphogenetic properties of microtubules and mitotic spindle assembly. *Cell* **9**, 401-410.

Illenberger S., Zheng-Fischhofer Q., Preuss U., Stamer K., Baumann K., Trinczek B., Biernat J., Godemann R., Mandelkow E. M. and Mandelkow E. (1998). The endogenous and cell cycle-dependent phosphorylation of tau protein in living cells: implications for Alzheimer's disease. *Mol. Biol. Cell* **9**, 1495-1512.

Kamimura, S. and Mandelkow, E. (1992). Tubulin protofilaments and kinesin-dependent motility. *J. Cell Biol.* **118**, 865-875.

Kanai Y. and Hirokawa N. (1995). Sorting mechanisms of tau and MAP2 in neurons: suppressed axonal transit of MAP2 and locally regulated microtubule binding. *Neuron* **14**, 421-432.

Khodjakov A., Lizunova E. M., Minin A. A., Koonce M. P. and Gyoeva F. K. (1998). A specific light chain of kinesin associates with mitochondria in cultured cells. *Mol. Biol. Cell* **9**, 333-343.

Klymkowsky, M. W. (1995). Intermediate filaments: new proteins, some answers, more questions. *Curr. Opin. Cell Biol.* **7**, 46-54.

Kumar J., Yu, H. and Sheetz, M. P. (1995). Kinectin, an essential anchor for kinesin-driven vesicle motility. *Science* **267**, 1834-1837.

Liao, G. and Gundersen, G. G. (1998). Kinesin is a candidate for cross-bridging microtubules and intermediate filaments. *J. Biol. Chem.* **273**, 9797-9803.

Lippincott-Schwartz, J. (1998). Cytoskeletal proteins and Golgi dynamics. *Curr. Opin. Cell Biol.* **10**, 52-59.

Lippincott-Schwartz, J., Cole, N. B., Marotta, A., Conrad, P. A. and Bloom, G. S. (1995). Kinesin is the motor for microtubule-mediated Golgi-to-ER membrane traffic. *J. Cell Biol.* **128**, 293-306.

Lopez, L. A. and Sheetz, M. P. (1993. Steric inhibition of cytoplasmic dynein and kinesin motility by MAP2. *Cell Motil. Cytoskel.* **24**, 1-16.

Mandelkow, E. and Mandelkow, E. M. (1995). Microtubules and microtubule-associated proteins. *Curr. Opin. Cell Biol.* **7**, 72-81.

Matus, A. (1994). Stiff microtubules and neuronal morphology. *Trends Neurosci.* **17**, 19-22.

Morris, R. L. and Hollenbeck, P. J. (1993). The regulation of bidirectional mitochondrial transport is coordinated with axonal outgrowth. *J. Cell Sci.* **104**, 917-927.

Morris, R. L. and Hollenbeck, P. J. (1995). Axonal transport of mitochondria along microtubules and F-actin in living vertebrate neurons. *J. Cell Biol.* **131**, 1315-1326.

Olson, K. R., McIntosh, J. R. and Olmsted, J. B. (1995). Analysis of MAP 4 function in living cells using green fluorescent protein (GFP) chimeras. *J. Cell Biol.* **130**, 639-650.

Paschal, B. M., Obar, R. A. and Vallee, R. B. (1989). Interaction of brain cytoplasmic dynein and MAP2 with a common sequence at the C-terminus of tubulin. *Nature* **342**, 569-572.

Prahlad V., Yoon M., Moir R. D., Vale R. D. and Goldman R. D. (1998). Rapid movements of vimentin on microtubule tracks: kinesin-dependent assembly of intermediate filament networks. *J. Cell Biol.* **143**, 159-170.

Presley, J. F., Cole, N. B., Schroer, T. A., Hirschberg, K., Zaal, K. J. and Lippincott-Schwartz, J. (1997). ER-to Golgi transport visualized in living cells. *Nature* **389**, 81-85.

Preuss, U., Döring, F., Illenberger, S. and Mandelkow, E.-M. (1995). Cell-cycle dependent phosphorylation and microtubule-binding of tau-protein stably transfected into chinese-hamster ovary cells. *Mol. Biol. Cell* **6**, 1397-1410.

Preuss, U., Biernat, J., Mandelkow, E.-M. and Mandelkow, E. (1997). The 'jaws' model of tau-microtubule interaction examined in CHO cells. *J. Cell Sci.* **110**, 789-800.

Ratner, N., Bloom, G. and Brady, S. (1998). A role for cyclin-dependent kinase(s) in the modulation of fast anterograde axonal transport: effects defined by olomoucine and the APC tumor suppressor protein. *J. Neurosci.* **18**, 7717-7726.

Rodionov, V. I., Gyoeva, F. K., Tanaka, E., Bershadsky, A. D., Vasiliev, J. M. and Gelfand, V. I. (1993). Microtubule-dependent control of cell-shape and pseudopodial activity is inhibited by the antibody to kinesin motor domain. *J. Cell Biol.* **123**, 1811-1820.

Rothman, J. E. (1994). Mechanism of intracellular protein transport. *Nature* **372**, 55-63.

Sato-Harada, R., Okabe, S., Umeyama, T., Kanai, Y. and Hirokawa, N. (1996). Microtubule-associated proteins regulate microtubule function as the track for intracellular membrane organelle transports. *Cell Struct. Funct.* **21**, 283-295.

Scales, S. J., Pepperkok, R. and Kreis, T. E. (1997). Visualization of ER-to-Golgi transport in living cells reveals a sequential mode of action for COPII and COPI. *Cell* **90**, 1137-1148.

Tanaka, Y., Kanai, Y., Okada, Y., Nonaka, S., Takeda, S., Harada, A. and Hirokawa, N. (1998). Targeted disruption of mouse conventional kinesin heavy chain, kif5B, results in abnormal perinuclear clustering of mitochondria. *Cell* **93**, 1147-1158.

Urbani, L. and Simoni, R. D. (1990). Cholesterol and vesicular stomatitis virus G protein take separate routes from the endoplasmic reticulum to the plasma membrane. *J. Biol. Chem.* **265**, 1919-1923.

Vallee, R. B. and Sheetz, M. P. (1996). Targeting of motor proteins. *Science* **271**, 1539-1544.

von Massow, A., Mandelkow, E.-M. and Mandelkow, E. (1989). Interaction between kinesin, microtubules, and microtubule-associated protein 2. *Cell Motil. Cytoskel.* **14**, 562-571.

Wacker, I., Kaether, C., Kromer, A., Migala, A., Almers, W. and Gerdes, H. H. (1997). Microtubule-dependent transport of secretory vesicles visualized in real time with a GFP-tagged secretory protein. *J. Cell Sci.* **110**, 1453-1463.

Wang Z., Khan S. and Sheetz M. P. (1995). Single cytoplasmic dynein molecule movements: characterization and comparison with kinesin. *Biophys. J.* **69**, 2011-2023.

Waterman-Storer, C. and Salmon, E. D. (1997). Microtubule dynamics: treadmilling comes around again. *Curr. Biol.* **7**, 369-372.

Weisshaar, B., Doll, T. and Matus, A. (1992). Reorganization of the microtubular cytoskeleton by embryonic microtubule-associated protein 2 (MAP2c). *Development* **116**, 1151-1161.

West, R. R., Tenbarge, K. M. and Olmsted, J. B. (1991). A model for microtubule-associated protein 4 structure. Domains defined by comparisons of human, mouse, and bovine sequences. *J. Biol. Chem.* **266**, 21886-21896.

Wiemer, E., Wenzel, T., Deerinck, T. J., Ellisman, M. H. and Subramani, S. (1997). Visualization of the peroxisomal compartment in living mammalian cells: dynamic behavior and association with microtubules. *J. Cell Biol*. **136**, 71-80.

Yoon M., Moir R. D., Prahlad V. and Goldman R. D. (1998). Motile properties of vimentin intermediate filament networks in living cells. *J. Cell Biol.* **143**, 147-157.